

Chemical reaction dynamics and relaxation phenomena in one component liquids, binary mixtures and electrolyte solutions

Biman Bagchi

Solid State and Structural Chemistry Unit, Indian Institute of Science, Bangalore 560 012, India and Jawaharlal Nehru Centre for Advanced Scientific Research, Bangalore 560 064, India

Our work in India in recent years has focused primarily on the following subjects: (a) Solvation and orientational dynamics in polar and non-polar liquids, (b) Vibrational energy and phase relaxation in liquids and gases, (c) Dynamics of freezing and glass transition, in particular anomalous relaxation in viscous liquids, (d) Electron transfer reactions in polar liquids, (e) Polymer and protein folding, (f) Viscosity and solvent dynamics effects on chemical reactions in solution, (g) Fluorescence resonance energy transfer (FRET) by Forster energy mechanism in polymers in solution, (h) Transport processes in liquids, including study of electrical conductivity in dilute electrolyte solution, and (i) Chirality-driven pattern formation in monolayers and bilayers. In this article we briefly review some of our work, we emphasize on the physical aspects and the relation with experimental results.

1. Introduction

The last two decades can be truly considered as the watershed years in the study of chemical dynamics in liquids¹⁻¹³. During these years, our understanding of solvent effects on chemical processes, on vibrational energy and phase relaxations, on orientational and dielectric relaxations and many other relevant problems increased many-folds and several of these areas can now be regarded as matured fields. This is to be contrasted with our limited understanding of liquid state dynamics in the sixties and seventies.

There are three main reasons for this great advance in our understanding of liquid phase dynamics. First, the rapid development in the laser and accompanying ultrafast spectroscopic techniques in seventies and eighties allowed increasingly shorter time resolution – this increased time resolution proved essential in the study of many chemical events⁵. Second, the theoretical formalism required to address the ultrafast relaxation of the solvent and the chemical reactions in general was

mostly developed between late fifties and early seventies when the time correlation function representation and projection operator technique became available¹⁴. Lastly, molecular dynamics simulations of realistic systems became increasingly possible from late seventies. Thus, many experimental results can be tested directly against simulations.

The advances in our understanding of solvent relaxation allowed in depth study of several related areas. For example, understanding of the dynamics of polar solvation allowed one to address the size dependence of limiting ionic conductivity^{12,13}. The latter in turn led to the development of molecular theories of the concentration and frequency dependence of ionic conductivity and viscosity of electrolyte solutions¹³. The study of solvation dynamics also allowed better understanding of solvent effects on electron transfer reactions¹⁵⁻²⁷.

The organization of the rest of the paper is as follows. In the next section we describe our past work on ion and dipolar solvation dynamics. In §3, we describe our work on electron transfer reactions. §4 contains discussion on vibrational phase and energy relaxation. §5 contains a discussion of our work on transport properties in binary mixtures. §6 contains discussion on re-entrant orientational relaxation in binary mixtures. §7 discusses work on heterogeneous dynamics in supercooled liquids. §8 contains our work on electrochemistry. §9 concludes with a brief discussion of ongoing and future projects.

2. Polar solvation dynamics

The most simple and straightforward way to study polar solvation dynamics is via time dependent fluorescence Stokes shift. In this experiment, a solute probe inside the polar solution is excited optically to its excited state which is characterized by a different charge distribution, resulting in a different dipole moment of the solute. This change in solute's dipole moment happens very fast, leaving the surrounding solvent molecules in the configuration still in equilibrium to the ground state charge distribution. Subsequently, the solvent molecules

e-mail: bbagchi@sscu.iisc.ernet.in

rotate and translate to solvate the new charge distribution, which leads to a lowering of the energy of the solute. The solute is so chosen that it has a long fluorescence lifetime. Thus, as the energy of the solute decreases due to stabilization by solvation, the fluorescence from the excited state undergoes a red shift. The physical scenario is illustrated in Figure 1.

The experimental studies have been carried out in many different laboratories around the world. The experimental results are usually expressed in terms of a non-equilibrium function, called solvation time correlation function, $S(t)$ which is defined by the following simple relation

$$S(t) = \frac{E_{\text{solv}}(t) - E_{\text{solv}}(t = \infty)}{E_{\text{solv}}(0) - E_{\text{solv}}(t = \infty)} \quad (1)$$

$S(t)$ so defined decays from unity to zero as time t varies from zero to infinity. Sometimes an alternative definition of solvation time correlation function is used, primarily by the theoreticians, based on the time correlation function formalism of statistical mechanics and random processes. Here the correlation function is denoted by $C_S(t)$ (to keep it distinct from $S(t)$) and is given by

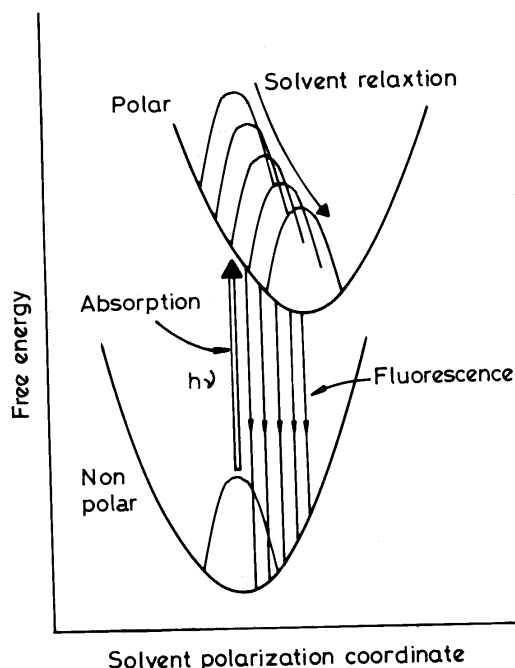


Figure 1. A schematic illustration of the physical process involved in the experimental study of solvation dynamics. The initial state is a nonpolar ground state. Laser excitation prepares it instantaneously in a charge transfer (CT) state which is polar. Initially, this CT state is a highly non-equilibrium state because at time $t = 0$, the solvent molecules are still in the Franck-Condon state of the ground state before the optical excitation. Subsequent solvation of the CT state brings the energy of the system down to the final equilibrium state which is detected by a red shift of the time-dependent fluorescence spectrum.

$$C_S(t) = \frac{\langle dE_{\text{solv}}(0)dE_{\text{solv}}(t) \rangle}{\langle dE_{\text{solv}}(0)dE_{\text{solv}}(0) \rangle}, \quad (2)$$

where $dE_{\text{solv}}(t)$ is the fluctuation in the solvation energy from its equilibrium value. It is assumed that $C_S(t)$ could be calculated with a given value of the solute dipole. The equality between $S(t)$ and $C_S(t)$ can hold if the solvent distortion by the newly created dipole is not significant. This is sometimes loosely referred to as the consequence of linear response of the solvent.

Many experimental and computer simulation studies have shown that solvents can broadly be divided into two categories: fast and slow. Water, acetonitrile, formamide and methanol fall under the first (that is, fast) category. These solvents show the presence of an ultrafast component which has a sub-100 fs time constant. For water and acetonitrile, this ultrafast component is found to carry more than 60% of the total solvation energy relaxation. This ultrafast decay is followed by a slow decay which could be larger than 1 ps. Many other liquids, including ethanol, propylene carbonate are among the solvents which are regarded as slow as these solvents do not seem to contain the ultrafast component. The decay here is typically non-exponential.

The first theoretical studies were based on continuum models which, for simplicity, assumed that the solute probe molecule can be approximated as a sphere with either a charge or a point dipole at the center of the molecule and the solvent was replaced by a dielectric continuum with a static dielectric constant ϵ_0 and an infinite frequency dielectric constant, ϵ_∞ . The relaxation of this dielectric continuum was assumed to be single exponential, with a time constant t_D , known as Debye relaxation time. Thus, the frequency (ω) dependence of the dielectric function, $\epsilon(\omega)$ is given by

$$\epsilon(\omega) = \epsilon_\infty + \frac{\epsilon_0 - \epsilon_\infty}{1 + i\omega t_D} \quad (3)$$

This simple continuum model predicts that solvation dynamics of an ion is single exponential with a time constant universally known as the longitudinal relaxation time, t_L , given by

$$t_L = \left(\frac{\epsilon_\infty}{\epsilon_0} \right) t_D \quad (4)$$

This simple expression gives rise to remarkable predictions for solvation times. For example, for water, t_D at 298 K is 8.3 ps, $\epsilon_0 = 78.5$ and $\epsilon_\infty = 4.86$, leading to a $t_L = 514$ fs which is already quite short. Experiments and computer simulations later found that solvation in water is much faster, even more than one order of magnitude faster than the prediction of the continuum model – but we shall come to that a bit later.

Experimental studies found that while the continuum model seems to provide nearly correct estimate of the rate of solvation for the slow liquids, shape of $S(t)$ is almost always markedly non-exponential. Several molecular theories have addressed this issue¹⁰⁻¹². A molecular hydrodynamic theory has been developed by us which attempts to explain the non-exponentiality as a consequence of length dependent relaxation in dipolar liquids. This length dependence is a consequence of spatial and orientational correlations present in a dense dipolar liquid – the continuum model result is recovered as the relaxation of the long wavelength polarization fluctuations. This length dependence is most simply described as the wavenumber (k) dependence of the longitudinal relaxation time, $t_L(k)$. Examples of the wavenumber dependence of the relaxation times are given in Figure 2. The relaxation times presented in this figure are obtained by solving the molecular hydrodynamic equations, derived by Chandra and Bagchi^{10,11}. There are certain notable features of this figure. First, the translational modes of the solvent have a strong influence on the relaxation times. This led to the conclusion that the translational modes can accelerate the decay of the large wavenumber modes, leading to a continuum model-like result. The relative weight of the

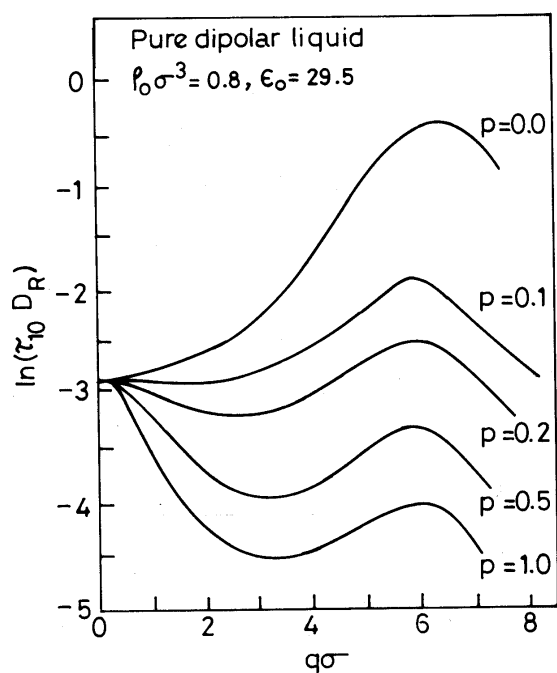


Figure 2. Effects of the solvent translational modes on the wave number (q) dependent longitudinal polarization relaxation time, $t_L(q)$. The values of the longitudinal relaxation time have been plotted as a function of the scaled wave number $q\sigma$, where σ is the diameter of a solvent molecule, for five different values of the translational parameter p which is a dimensionless ratio of the translational to the rotational diffusion coefficients of the solvent molecule. The values of the reduced density and the dielectric constant are shown on the figure. For details, see refs 10, 11.

translational mode is determined by two factors. First, the dimensionless quantity, p which is equal to $D_T/2D_R\sigma^2$, where D_T and D_R are the translational and rotational diffusion coefficient of the solvent molecules, while σ is the molecular diameter of the solvent. A value of p above 0.5 was found to reduce the contributions of the large wave numbers, and hence of correlations significantly. Second, the more dipolar the solvent molecule is, the larger the effects of orientational correlations, and the larger is the magnitude of the relaxation time at intermediate wave numbers (where $k\sigma \approx 2p$).

The molecular hydrodynamic theory could provide an explanation of the observed non-exponentiality in terms of a simple picture. However, this simple picture breaks down for fast liquids. It was found that these liquids (water, acetonitrile, methanol) exhibit more complex dynamics because of factors which are unique to each. The molecular hydrodynamic theory was generalized to include memory or non-Markovian effects by several groups¹². It was found that the ultra-fast Gaussian component in the solvation dynamics of water was mainly due to the high frequency modes. The two modes which play important role are the inter-molecular vibration at 200 cm^{-1} and the libration at 685 cm^{-1} . The solvation time correlation function of an ion is shown in Figure 3. In the case of acetonitrile, the underdamped rotational motion was found to be the main reason, while for methanol (which shows smaller amplitude of the inertial component), it is again the libration mode which is responsible for the ultrafast solvation. Although there are differences in the language among various theories, there is a broad consensus regarding the origin of the ultrafast solvation in these liquids.

3. Solvent effects on electron transfer reactions in solution

Electron transfer reactions are ubiquitous in chemistry. The standard description of electron transfer reactions start with the Marcus theory which provided a language to describe the rates of these reactions in terms of reorganization energy and the free energy of reaction^{1,15,16}. In the simplest description, the reactant and the product are described by two potential energy surfaces with the solvation energy as the reaction coordinate. In the case of a non-adiabatic reaction (when the electronic coupling, V_{el} between the reactant and the product is very small), the solvent dynamics effects are small. In the other extreme is the adiabatic reaction where the electronic coupling between the two participating surfaces (donor and acceptor) is so strong that the electron transfer occurs on one surface which is formed due to mixing of the two surfaces. The solvent dynamic effect is believed to be strong in the adiabatic limit. The most electron transfer reactions fall in between

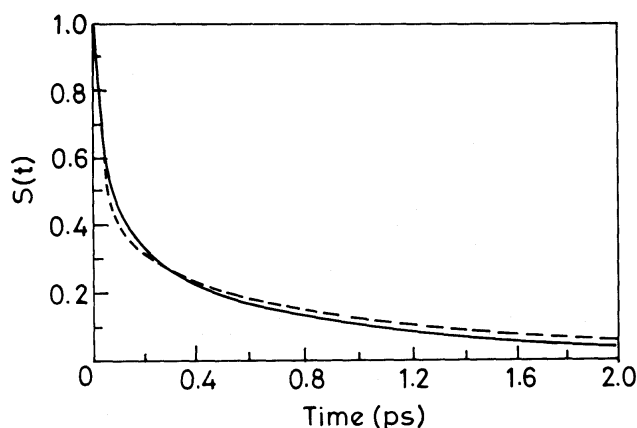


Figure 3. Comparison between the theoretical prediction (the solid line) with the experimental results (the dashed line) of the solvation dynamics in liquid water. The theoretical calculation contains contributions from both the rotational and the intermolecular vibrational modes of the liquid.

the two limits and are sometimes referred to as weakly adiabatic reaction. A modest degree of solvent dynamic effect is expected for weakly adiabatic reactions¹⁷.

The theoretical treatments of solvent effects on weakly adiabatic reaction have followed two different approaches. One is to treat the reaction as non-adiabatic and use Fermi Golden rule expression to formulate the rate. The initial approach of Marcus and others has been extended greatly by Jortner and Bixon²¹⁻²⁴ who showed how to include the effects of intra-molecular vibrational modes which not only minimize the effects of solvent polarization mode but can also enhance the rates of electron transfer. In particular, for the reactions in the Marcus inverted regime, the participation of intra-molecular vibrational modes can increase the rate by many orders of magnitude.

We have studied the effects of ultrafast solvation on electron transfer reaction within the one-dimensional Marcus model and also the more general Jortner-Bixon multidimensional description. In the previous case, we used a non-Markovian generalization of the energy diffusion model employed earlier by Zusman¹⁸. In this non-Markovian description (proposed first by Hynes¹⁹), the frequency dependent friction is obtained directly from the time dependent solvation time correlation function, by using the following reaction

$$S(z) = \frac{z + \mathbf{z}(z)}{\mathbf{w}_0^2 + z\mathbf{z}(z) + \mathbf{z}(z)^2}, \quad (5)$$

where $\mathbf{z}(z)$ is the frequency (z) dependent friction on electron transfer and \mathbf{w}_0 is the harmonic frequency of the reactant surface. This is also known as solvation frequency¹⁹.

We have used our molecular hydrodynamic theory to calculate $S(z)$ and then extract the frequency dependent friction, for electron transfer in water, acetonitrile and

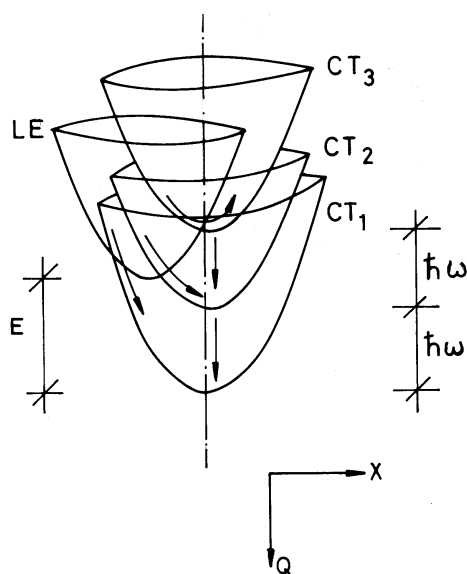


Figure 4. A general two-dimensional multisurface schematic representation of electron transfer reaction in the Marcus inverted region. LE and CT_1 , CT_2 , CT_3 ... are the effective potential energy surfaces for the reactant (which is the locally excited) state, and the product vibrational states. LE is the electron donor and the CT states are the electron acceptor. X and Q are the two classical vibrational degrees of freedom and ω is the vibrational frequency of the quantum degree of freedom. E is the energy gap between the minimum energies of the donor and the acceptor states.

methanol, for both weakly adiabatic reaction and also for non-adiabatic reaction. The important result was that due to the presence of the ultrafast component, no solvent dynamic effect on the barrier crossing dynamics was predicted by the theory. Therefore, within the one-dimensional Marcus model, the ultrafast solvation removes dynamic effects effectively and the original prediction of Zusman of the inverse dependence of the ETR rate on the longitudinal relaxation time, $\tau_L (= \langle \mathbf{e}_\infty / \mathbf{e}_0 \rangle / \tau_D)$ which itself is proportional to solvent viscosity, is not valid²⁷⁻²⁹. To summarize, no significant solvent dynamic effects are predicted by theory for ultrafast solvents.

We have also investigated the role of solvation dynamics in the most general multidimensional Jortner-Bixon model. A schematic illustration of the model is given in Figure 4. We have generalized the existing formalism to include the effects of back reaction and the vibrational energy relaxation^{27,30}. The existing theoretical formulations of electron transfer reactions (ETR) neglect the effects of vibrational energy relaxation (VER) and do not include higher vibrational states in both the reactant and the product surfaces. Both of these aspects can be important for photo-induced electron transfer reactions, particularly for those which are in the Marcus inverted regime. We have developed a theoretical formulation which includes both these two aspects. The formalism requires an extension of the hybrid model introduced earlier by Barbara *et al.*³¹. We model

a general electron transfer as a two-surface reaction where overlap between the vibrational levels of the two surfaces create multiple, broad reaction windows. The strength and the accessibility of each window is determined by many factors. We find that when VER and reverse transfer are present, the time dependence of the survival probability of the reactant differs significantly (from the case when they are *assumed* to be absent) for a large range of values of the solvent reorganization energy (I_x), quantum mode reorganization energy (I_q), electron coupling constant (V_{el}) and vibrational energy relaxation rate (k_{VER}). Several interesting results, such as a transient rise in the population of the zeroth vibrational level of the reactant surface, a Kramers (or Grote-Hynes) type recrossing⁷ due to back reaction and a pronounced role of the initial Gaussian component of the solvation time correlation function in the dynamics of electron transfer reaction, are observed³⁰. Significant dependence of the electron transfer rate on the ultrafast Gaussian component of solvation dynamics is predicted for a range of values of V_{el} , although dependence on average solvation time can be weak. Another result is that, although VER alters relaxation dynamics in both the product and the reactant surfaces noticeably, the average rate of electron transfer is found to be weakly dependent on k_{VER} for a range of values of V_{el} ; this independence breaks down only at very small values of V_{el} . In addition, the hybrid model is employed to study the time resolved fluorescence line shape for the electron transfer reactions. It is found that VER can have a significant effect on emission lineshape³⁰.

4. Vibrational relaxation

The study of vibrational relaxation is a subject of great importance in physical chemistry^{32,33}. There are two different processes that are studied in this area. One is the vibrational phase relaxation and the other is the vibrational energy relaxation. Below we briefly discuss both the two relaxation processes.

4.1 Vibrational phase relaxation

Vibrational phase relaxation is discussed in terms of the Kubo model where the controlling mechanism giving rise to the loss of the phase of a coherently excited oscillators is by modulation of the vibrational frequency, ω_0 (ref. 32). Early theoretical and experimental studies found a dependence of the phase relaxation rate on viscosity. Early studies also assumed a quadratic dependence of the vibrational rate on the quantum number of the overtone for overtone dephasing. However, recent experimental studies³⁴ showed a sub-quadratic, almost linear dependence of the dephasing rate on the quantum number of the overtone.

Our studies showed that the sub-quadratic quantum number dependence can be explained in terms of the biphasic response of the liquid³⁵. In particular, the inertial component of the frequency modulation time correlation function was shown to play an important role. The reason has a simple picture. As the quantum number increases, the faster response is probed which is more likely to be in the inertial regime.

We have also studied the anomalous rise in the phase relaxation time in nitrogen as the critical point is approached along the phase coexistence line. It was proposed that the anomalous rise is due to the enhanced contribution from the rotational-vibrational coupling which makes small contribution in the liquid phase but becomes increasingly important as the gas phase is approached³⁶. A comparison between the theoretical and the experimental results is shown in Figure 5.

4.2 Vibrational energy relaxation

The study of vibrational energy relaxation (VER) forms an essential part of physical chemistry and has a long history^{31,32}. This long interest in VER comes from the critical role that it plays in chemical reactions. However, it was not easy to obtain information about the rates of vibrational energy relaxation in a bond. Study of VER gained momentum after laser spectroscopy allowed measurement of population of vibrational levels. Theoretical studies on vibrational energy relaxation have mostly been carried out by invoking two basic models – the isolated binary collision (IBC) model³⁶ in

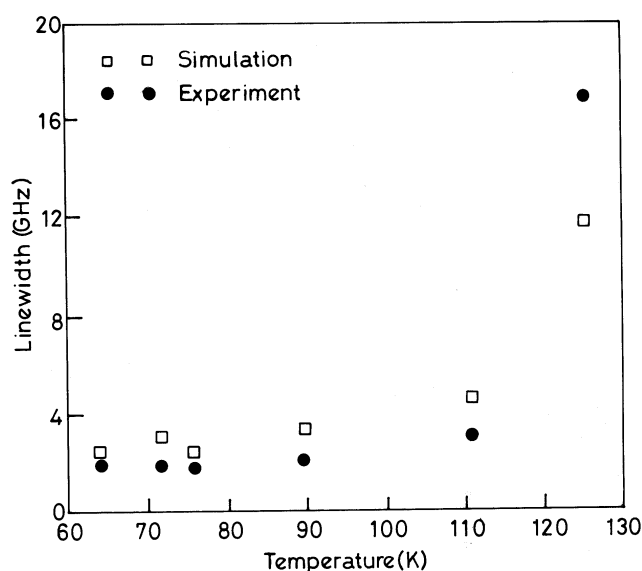


Figure 5. Temperature dependence of the rate of vibrational phase relaxation in liquid nitrogen as the temperature is varied along the phase coexistence line towards the critical point. The graph compares the simulated linewidth of the isotropic Raman linewidth with that of the experimental one. The critical temperature is 125.3 K.

which the collision frequency is modified by the liquid structure, and the weak coupling model³¹ where the vibrational motion of the molecule weakly couples to the rest (translational and rotational) degrees of freedom so that a perturbative technique can be employed.

The IBC model was developed by Herzfeld *et al.*³⁷. In this model, one starts with the assumption that the VER rate for a two-level system can be given by

$$\mathbf{t}_{ij}^{-1} = P_{ij} \mathbf{t}_c^{-1}, \quad (6)$$

where \mathbf{t}_c^{-1} is the collision frequency and P_{ij} is the probability per collision that a transition from level 'i' to level 'j' will take place. P_{ij} is independent of density but does depend on temperature whereas \mathbf{t}_c depends on both these state parameters. In the gas phase, \mathbf{t}_c can be obtained from kinetic theory, but it is difficult to obtain in the condensed phase. If the colliding molecules are approximated by effective hard spheres with radius \mathbf{s} , then an expression for the collision frequency can be obtained from the Enskog theory which gives the frequency as proportional to $g(\mathbf{s})$ where $g(\mathbf{s})$ is the value of the radial distribution function at contact. \mathbf{t}_c is also proportional to the friction and hence to the viscosity of the gas. Thus, the IBC model with Enskog collision frequency predicts a rate proportional to the viscosity of the gas. The point of interest here is that till recently there did not exist any reliable calculation of the binary friction *in a dense liquid* within the Enskog theory for a continuous potential.

The second line of approach considered the vibrational energy relaxation as a classical process where energy is dissipated to the medium by the usual frictional process. Then, one can adopt a stochastic approach. For VER involving low frequencies, it is reasonable to assume that the vibration is harmonic. Under this condition, one can write a generalized Langevin equation of motion for the normal coordinate $Q(t)$ as³⁸⁻⁴⁰

$$m\ddot{Q}(t) = -m\bar{\omega}^2 Q(t) - \int_{-\infty}^t dt' \mathbf{z}_{\text{bond}}(t-t') \dot{Q}(t') + R_Q(t), \quad (7)$$

where m is the reduced mass of the diatomic comprising the vibrating bond and $\bar{\omega}$ is the renormalized bond frequency which is shifted from the bare bond frequency due to the presence of solvent molecules⁴⁰, $\zeta_{\text{bond}}(t)$ is the time dependent bond friction coefficient, and $R_Q(t)$ is the random force related to $\mathbf{z}_{\text{bond}}(t)$ by the fluctuation-dissipation theorem. The following important observation is made at this point. Even at as low a bond frequency as 100 cm^{-1} , the solvent frictional force on the bond is very small. Thus, while the zero frequency friction can be large, the relaxation of Q probed at large frequency can be in the underdamped limit.

The rate of the VER, $1/T_1$, of a classical oscillator is given by the simple Landau-Teller expression³⁸⁻⁴⁰,

$$\frac{1}{T_1} = \frac{\mathbf{z}_{\text{bond}}(\bar{\omega})}{m}, \quad (8)$$

where $\mathbf{z}_{\text{bond}}(\bar{\omega})$ is the Fourier-Laplace transform of $\mathbf{z}_{\text{bond}}(t)$. This friction is responsible for population redistribution in vibrational levels since energy dissipates through this friction.

The molecular dynamics simulation studies of Berne *et al.*³⁹ have shown that if a homonuclear diatomic consisting of the same atoms as the surrounding solvent is not allowed to rotate, then $\mathbf{z}_{\text{bond}}(\bar{\omega})$ could be approximated as

$$\mathbf{z}_{\text{bond}}(\bar{\omega}) = \frac{\mathbf{z}(\bar{\omega})}{2}, \quad (9)$$

where $\mathbf{z}(\bar{\omega})$ is the friction experienced by one of the atoms of the vibrating homonuclear diatomic. Eq. (9) was also used by Oxtoby in his theory of vibrational dephasing³². Eq. (9) gives a simple way to relate the solvent dynamic response to the VER rate. The above expression is semi-quantitatively reliable, so is the Landau-Teller expression, at least for the low frequency mode. Therefore, the success of the weak coupling method depends on an accurate frequency dependent friction. However, analytic calculation of frequency dependent friction has been a difficult task and several different approximations have been used. The most successful is the scheme used by Egorov and Skinner³⁸ who fitted a short time expansion to a $\cos(at)/\cosh(bt)$ form where the constants a and b are obtained from the second and fourth time derivative of the force-force time correlation function at time $t = 0$. The other method is the instantaneous normal mode (INM) analysis which has also been fairly successful in getting the high frequency response of the liquid³⁹. We have used a mode coupling theory approach to calculate the high frequency response of the frictional force⁴¹. The agreement of this approach with simulations is comparable to the INM.

In a recent paper⁴² we have presented a novel method to obtain an Enskog level description of binary friction of continuous potential. Numerical implementation of this new method gave excellent agreements of the time-dependent friction and self-diffusion coefficient with simulation results.

The new Enskog theory was used to calculate the frequency-dependent binary friction for fluids interacting with the Lennard-Jones potential. We use this friction to calculate the rate of the vibrational energy relaxation and compared the theoretical result with available simulation data. The agreement between the theory and

simulation is found to be satisfactory⁴¹. In a sense, this work can be regarded as an amalgamation of IBC and the Landau–Teller approach to VER.

Another interesting aspect of this work is the fact that the frequency-dependent binary friction $\zeta_E(\omega)$ shows an interesting frequency dependence with a hump at low frequency, which has already been seen in many simulation studies. This interesting aspect of frequency dependence of friction is shown in Figure 6 where the simulation results of Berne *et al.* have been compared with our new Enskog calculation. We regard this hump describing the cross-over frequency below which the collective effects become important⁴³.

We have also used mode coupling theory to study vibrational energy relaxation in dense liquids⁴². This work also showed that VER is dominated by the binary component of friction.

5. Transport coefficients in binary mixtures

Binary mixtures are ubiquitous in chemistry. Most of the chemical solvents are multi-component and in particular binary. In a binary mixture, by altering the composition of one of the ingredients, one can change solubility, polarizability, viscosity and many other static and dynamic properties. This tunability is of great use in chemistry. Although the static and dynamic properties of many mixtures are well characterized, a

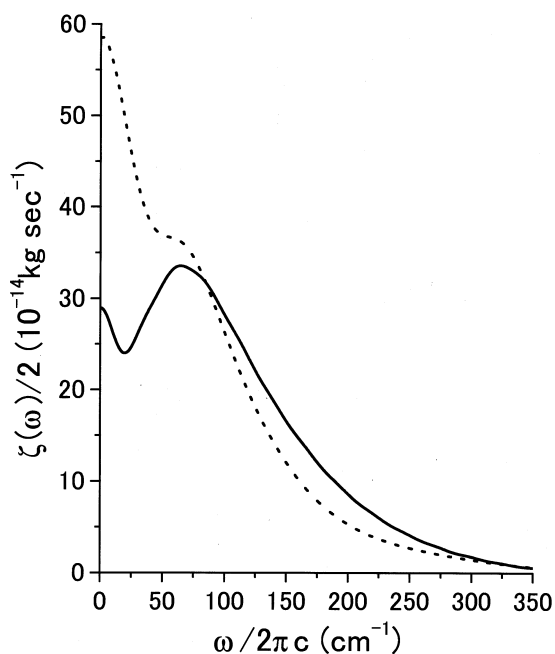


Figure 6. The real part of the frequency dependence of friction on a solvent atom calculated from the Enskog theory (solid line), compared with the simulated one (the dashed line). Note the hump near 60 cm^{-1} (ref. 42).

general theoretical framework to understand especially the dynamical properties is still lacking.

The elegant theory of Kirkwood and Buff can be used to explain many aspects of static properties⁴⁴ but the same is not available for the dynamical properties. This is somewhat surprising, given the fact that the dynamical properties in a binary mixture show exotic features which pose interesting challenges to theoreticians. Among them the extrema observed in the composition dependence of excess viscosity^{45,46}, the anomalous viscosity dependence of the rotational relaxation time⁴⁷ and the heterogeneous dynamics near glass transition are certainly the very important ones. Highly non-exponential solvation dynamics have been observed in binary dipolar mixtures^{48,49}. In recent years, a large number of studies have been devoted to glass transition and glassy behaviour in binary mixture on Kob–Andersen model^{50,51} but with a single composition $x_A = 0.8$ and $x_B = 0.2$ (refs 52, 53). None of these studies has addressed the well known anomalous composition dependence.

In a binary mixture there involves the choice of three different interactions, two length scales and two different masses. A combination of all these different parameters gives rise to several microscopic time scales in the system. Thus the equilibrium and dynamical properties in these systems are considerably different from that of a one-component system. In addition to the multiple time scales, binary mixtures have interesting relaxational dynamics which are controlled not only by density and momenta relaxation but also by the composition fluctuation, which plays an important role. This is particularly true when interaction energies between the two constituents and also the sizes differ significantly. If the free energy cost of composition fluctuation is not very large then it becomes a convenient channel for stress and other relaxation. The composition fluctuation can also be rather slow as it involves exchange of atoms. Given the diversity present in the system it is naive to expect any simple theory to explain the anomalies present in a binary mixture. In fact, very little understanding of a binary mixture is possible by studying a one-component system.

In this section we address the above-mentioned anomalies present in the binary mixture. In addition to this we will also present a study of the probability of composition fluctuation in a binary mixture^{54–56}. To capture the various aspects of composition dependence of viscosity, we have introduced two new models (subsequently called as model I and model II). Model I is an attractive or structure making model owing to the most strong interaction between two different species of the binary mixture whereas model II is of repulsive or structure breaking kind as the different species have least interaction between them. We carried out both mode coupling theory (MCT) calculation and (NVE)

and (NPT) simulation on the two above models to show that even the very two simple models as above can contain the anomalous composition dependence of viscosity. The composition fluctuation is studied from (NVE) molecular dynamics simulation results. (NPT) molecular dynamics simulation of Gay–Berne ellipsoids in a Lennard–Jones binary mixture is performed to study the anomalous viscosity dependence of the orientational relaxation⁵⁷. We showed that the orientational relaxation time has a re-entrant viscosity dependence for different composition which tells in a dramatic fashion that *viscosity is not an unique determinant of relaxation time*. A similar system of Gay–Berne ellipsoids in a binary Lennard–Jones mixture is used to study the heterogeneous orientational dynamics⁵⁸. The parameters in the binary system in this study is the same as Kob–Andersen model. In this system at high pressure the orientational relaxation dynamics is indeed heterogeneous.

5.1 Non-ideal composition dependence of viscosity: correlation between excess viscosity and excess volume

It is generally believed that the total viscosity increases on mixing if the two different species of a binary mixture attract each other and decreases when the different ingredients of the mixture repel each other. In a real mixture an observed property P is often very different from its predicted ideal value P_{id} given by⁵⁴,

$$P_{id} = x_A P_A + x_B P_B, \quad (10)$$

where x_A and x_B are the mole fractions and P_A and P_B are the values of the property P of the corresponding pure (single component) liquids. Now we define the corresponding excess quantity P_{excess} as,

$$P_{excess} = P - P_{id}. \quad (11)$$

These quantities, i.e. P and P_{excess} can be any dynamic or static quantities such as viscosity (\boldsymbol{h}), specific heat, volume, etc. Departure from eq. (10) is attributed to the specific interaction between the two components in the mixture. While the reason for this deviation is often discussed in terms of the above-mentioned attraction or repulsion between the constituents, quantitative understanding of these phenomena from microscopic theory has remained largely incomplete. In order to address this problem, we constructed two different binary mixture models (referred to as model I and model II) in which the solute–solvent interaction strength is varied by keeping *all the other parameters* unchanged⁵⁴. All the three interactions are described by either the Lennard–Jones or the modified Lennard–Jones potential. In

model I, specific structure formation between solute and solvent molecules is mimicked by stronger solute–solvent attractive interaction ($\boldsymbol{e}_{AB} = 2.0$) than that between solvent–solvent ($\boldsymbol{e}_{AA} = 1.0$) and solute–solute ($\boldsymbol{e}_{BB} = 0.5$) interactions. The second model (model II) involves structure-breaking by weak solute–solvent interaction ($\boldsymbol{e}_{AB} = 0.3$). These two models are perhaps the simplest to mimic the structure making and structure breaking in binary mixtures⁵⁴. For convenience, we denote the solvent molecules as A , and the solute molecules as B . In both the models, A and B have the same radii and same masses. In this section, we carry out both MCT calculation and extensive (NVE) and (NPT) molecular dynamics simulations to evaluate the non-ideality in the composition dependence of viscosity and we have also established the correlation between excess volume (Vol_{excess}) and excess viscosity (\boldsymbol{h}_{excess}) throughout the composition range for both the models. Note that the latter part needs the simulation to be carried out through (NPT) ensemble method as (NVE) simulation does not allow volume fluctuation. Note that, MCT calculations for one-component systems have been extensively studied earlier⁵⁹.

5.2 Results and discussion

Figure 7 depicts the non-ideality of viscosity obtained from both (NVE) simulation and mode coupling theory with respect to solute (B) composition, for both the models. Though the agreement between theory and simulation is certainly not perfect, the trends are similar in both the calculations. Note that the theoretical calculation does not use *any* simulation data as input or *any adjustable parameter* either; thus the theory and the simulation provide independent tests of each other which is important for binary mixtures^{53–55}.

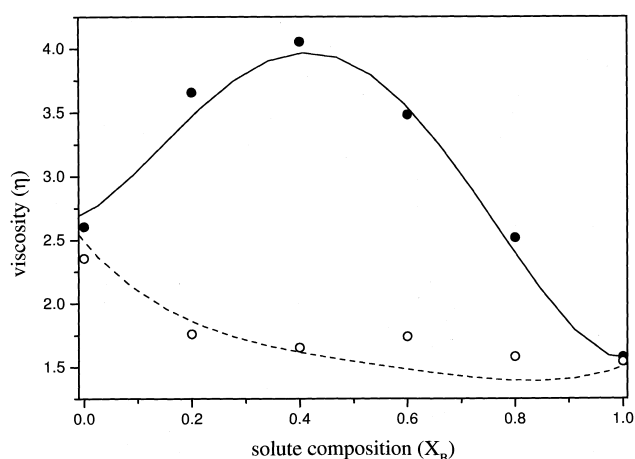


Figure 7. The composition dependence of viscosity obtained from (NVE) MD simulations (symbols) and mode coupling theory (lines) for models I and II (the attractive and the repulsive models, respectively). Filled (open) circles show simulation results for model I (model II). The lines show the prediction of the theory.

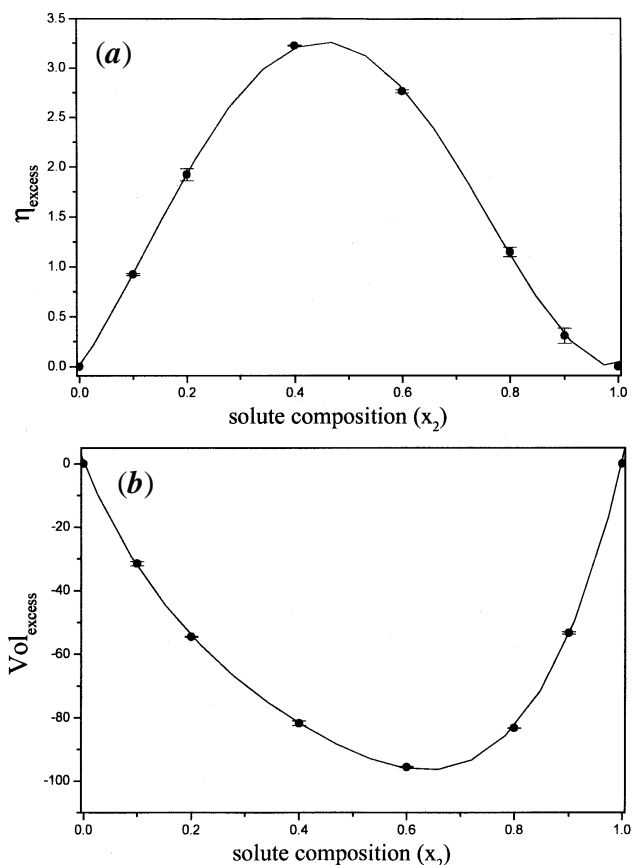


Figure 8. Composition dependence of excess viscosity and excess volume for model I. In (a), the calculated excess viscosity (η_{excess}) is plotted against solute composition (x_B) for model I. In (b), the variation of excess volume ($\text{Vol}_{\text{excess}}$) with solute composition (x_B) is plotted for the same model. The solid lines are for the guidance to the eye.

Figures 8 and 9 show the correlation between excess volume and excess viscosity given by eq. (11). The results of these figures are drawn out from (NPT) simulation as (NVE) simulation does not allow volume change.

Figure 7 shows the positive deviation of viscosity and negative deviation of volume from their ideal value for model I. Figure 8a, on the other hand, shows negative deviation of viscosity and Figure 8b shows positive deviation of volume in case of model II. Note the correlation between excess volume and excess viscosity is always opposite and in two different models they manifest in opposite ways. The results presented in Figures 7–9 can be partly understood by analysing the microscopic structure. As the solute–solvent interaction strength affects the structure surrounding a solute/solvent to a great extent^{60,61}, the above observed features are reflected in the *increment of correlation among the unlike species*, $g_{AB}(r)$, for model I while the reverse is seen for model II. We can refer to such behaviour as the ‘structure forming’ for model I and ‘structure breaking’ in model II.

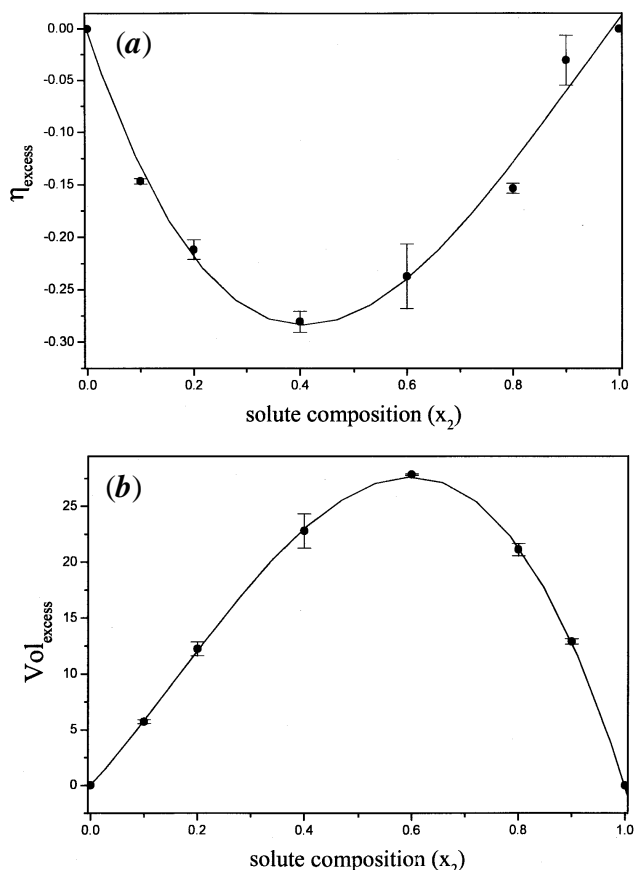


Figure 9. Composition dependence of excess viscosity and excess volume for model II. In (a), the excess viscosity (η_{excess}) is plotted against solute composition (x_B) for model II. In (b), excess volume ($\text{Vol}_{\text{excess}}$) is plotted against the solute composition (x_B) for model II. Similar to Figure 8, solid lines are only for guidelines.

The above figures can explain the complex phenomena of non-ideality in dynamic properties from very simple microscopic models which explain that the key to the non-ideality of mixtures belongs to the nature of interaction between the different species constituting the mixture.

6. Re-entrant orientational relaxation in binary mixtures

Conventionally, the rotational diffusion (D_R) coefficient of a solute is given by the well known Debye–Stokes–Einstein (DSE) relation,

$$D_R = \frac{k_B T}{8\pi h r_s}, \quad (12)$$

where $k_B T$ is the Boltzmann constant times the temperature (T), h is the viscosity of the liquid medium and r_s is the radius of the molecule. Experimentally, one measures the orientational time correlation function $C_l(t)$

(ℓ is the rank of the spherical harmonic coefficients), with $\ell = 1$ or 2. Now if the Debye rotational diffusion model is assumed, then the relaxation time $t_{\ell R}$ is given by,

$$t_{\ell R} = [\ell(\ell + 1)D_R]^{-1}, \quad (13)$$

where D_R is the rotational diffusion coefficient. Thus, according to the hydrodynamic theory the viscosity is a unique determinant of the rotational relaxation time. As discussed in the Introduction, there exists multiple time scale in a binary mixture. Given the diversity present in the system, it is naïve to expect a simple proportionality between $t_{\ell R}$ and η to hold.

The breakdown of the hydrodynamic theory was dramatically exhibited by Beddard *et al.*⁴⁷. They used picosecond fluorescence depolarization technique to study the rotational relaxation time of dye cresyl violet in ethanol–water mixture by varying the ethanol–water composition. They reported different rotational relaxation times in solutions at the same viscosity but different compositions.

This re-entrance type behaviour of the orientational relaxation time when plotted against viscosity is yet to be explained. Although the viscosity itself in a binary mixture is known to exhibit non-ideal behaviour (as has been discussed in the previous section) it should be noted that the composition dependence of the orientational relaxation time cannot be understood only in terms of this non-ideality in viscosity. The re-entrance is strongly dependent on the specific interaction of the solute with the solvents which has already been discussed by Beddard *et al.*⁴⁷. The role of specific interaction in the orientational dynamics has often been discussed and the effect has been included in the DSE relation by changing the boundary condition⁵. However, to the best of our knowledge, a detailed study of the rotational dynamics in a binary mixture has not been carried out before.

Extensive MD simulations at constant pressure (P), temperature (T) and total number of molecules (N) have been carried out to study the orientational relaxation of prolate ellipsoids in several binary mixtures. The interaction potentials used in this study are well behaved and have been studied earlier^{62,63}. We find that the orientational relaxation time of the ellipsoid when plotted against the solvent viscosity, does indeed show a re-entrance.

The re-entrance behaviour is shown in Figure 10. Here the rotational relaxation time is plotted against the viscosity by varying the composition. The maximum of viscosity is obtained at composition 0.4 where its value is 2.66 times the value at $c_B = 0$. The rotational relaxation time varies by a factor of 1.5. The essence of re-entrance is nicely captured in Figure 10.

Note that although Figure 10 has the same qualitative feature as the experimental plot⁴⁷, there exist some differences in the intrinsic details. The details of the plot can be easily altered by tuning the interactions⁵⁷.

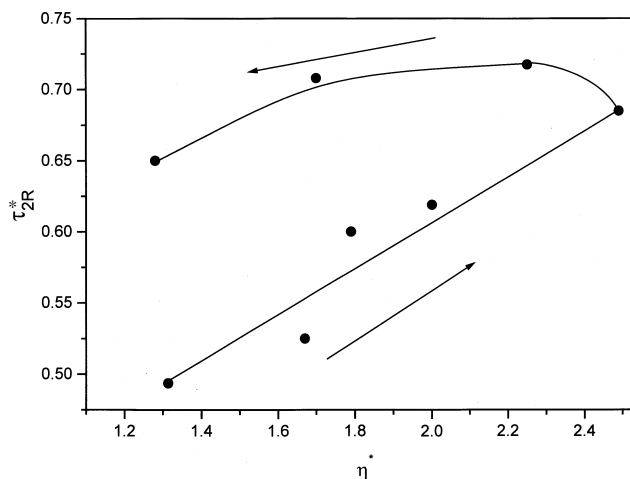


Figure 10. The reduced orientational relaxation time, t_{2R} , plotted against the reduced viscosity of the binary mixture, η , is shown by the filled circles, t_{2R} shows a re-entrance. The solid line is a guide to the eye. The compositions of the solvent are 0.04, 0.08, 0.15, 0.2, 0.4, 0.6, 0.8 and 1.0 where the direction of the arrows show the increasing composition of (B) particles. The study is performed at $T^* = 1.0$ and $P^* = 1.0$.

We have investigated whether the non-ideality in viscosity alone can reproduce the observed re-entrance in orientational relaxation time. We found the answer to be in the contrary – *the non-ideality in viscosity in a binary mixture cannot alone explain the re-entrance*⁵⁷.

The study here shows that in a system where the solute interacts with the two different species in a binary mixture in a different manner, its rotational relaxation will depend more on the composition than on the viscosity of the binary mixture. Thus, the re-entrant type behaviour is strongly dependent on the interactions of the solute with the two different species in the solvent.

7. Heterogeneous dynamics in supercooled liquid

Recent experiments, simulations and theoretical studies all seem to suggest the presence of heterogeneous dynamics in a supercooled liquid⁶⁴. This heterogeneity in the kinetics is believed to have originated from the free energy landscape with multiple minima and maxima^{52,65}. Although many characteristics of the free energy functional have been qualitatively calculated from the q spin Potts model⁶⁶, the connection between the dynamics and the free energy landscape is not fully clear. Even the nature of the heterogeneity (entropic or density) is not understood yet⁶⁷.

The most direct experimental evidence of the heterogeneous relaxation comes from the NMR and fluorescence depolarization study of the tagged probes in supercooled liquids⁶⁴. These experiments measure translational and orientational relaxation of the probe molecules. The advantages of using the orientational

relaxation as a probe of heterogeneity are many fold. First, the orientational relaxation is mostly a local phenomenon and thus explores only the local dynamics. Second, the orientational relaxation is faster than the density relaxation, therefore the density relaxation and orientational dynamics are well separated in time.

Here we present an (NPT) MD simulation study of the orientational relaxation of a tagged solute in a model, supercooled, binary mixture⁵⁸. The study shows the presence of widely different orientational dynamics of the solutes in different locations in the same solvent.

7.1 Results and discussions

In Figure 11 we show the orientational time correlation function of the 4 tagged ellipsoids located at different regions. The figure clearly shows the presence of heterogeneous dynamics in the supercooled liquid as probed by the orientational dynamics of the ellipsoids. The initial decay of the orientational time correlation function (OCF) of all the 4 ellipsoids (till $C_{2R}(t) = 0.9$), due to their inertial motion, is similar. However, after this initial decay, the orientational time correlation function of all the particles behaves differently. OCF of particle 1, 3, and 4 decays with different time scales. On the other hand, the orientational time correlation function of particle 2 seems to saturate after decaying to 0.7.

This implies the existence of two different dynamic regions even within such a small system.

In order to further investigate the nature of these regions, we have calculated two particle radial distribution functions, individually, for all the four ellipsoids. The radial distribution functions show that particle 3 has the maximum number of neighbouring (A) particles. The (B) particles surrounding ellipsoid 3 are mostly at a distance, $r = 1.5 \sigma$. Thus, the (B) particles are positioned mostly at the tip of the ellipsoid 3. Since the (B) particle is smaller than the ellipsoid, its dynamics takes place at a smaller time scale. On the other hand, the dynamics of the larger (A) particle is much slower than the rotational dynamics of the ellipsoid. As the rotation of the ellipsoid is facilitated when there are more mobile particles on its sides rather than at the tips, the presence of more number of (A) particles around ellipsoid 3 hinders its rotational motion.

Thus we can argue that at the pressure and temperature we have studied and within 1.2 ns time, the (A) particles are almost frozen but the (B) particles are mobile. This is similar to the prediction of Bosse *et al.*⁶⁸ who performed a mode coupling theoretical calculation of binary mixture of disparate size and have shown that although the larger particles form a glass, the smaller particles remain mobile.

The picture might be different for different probes. If the solute is large and massive then its time scale of

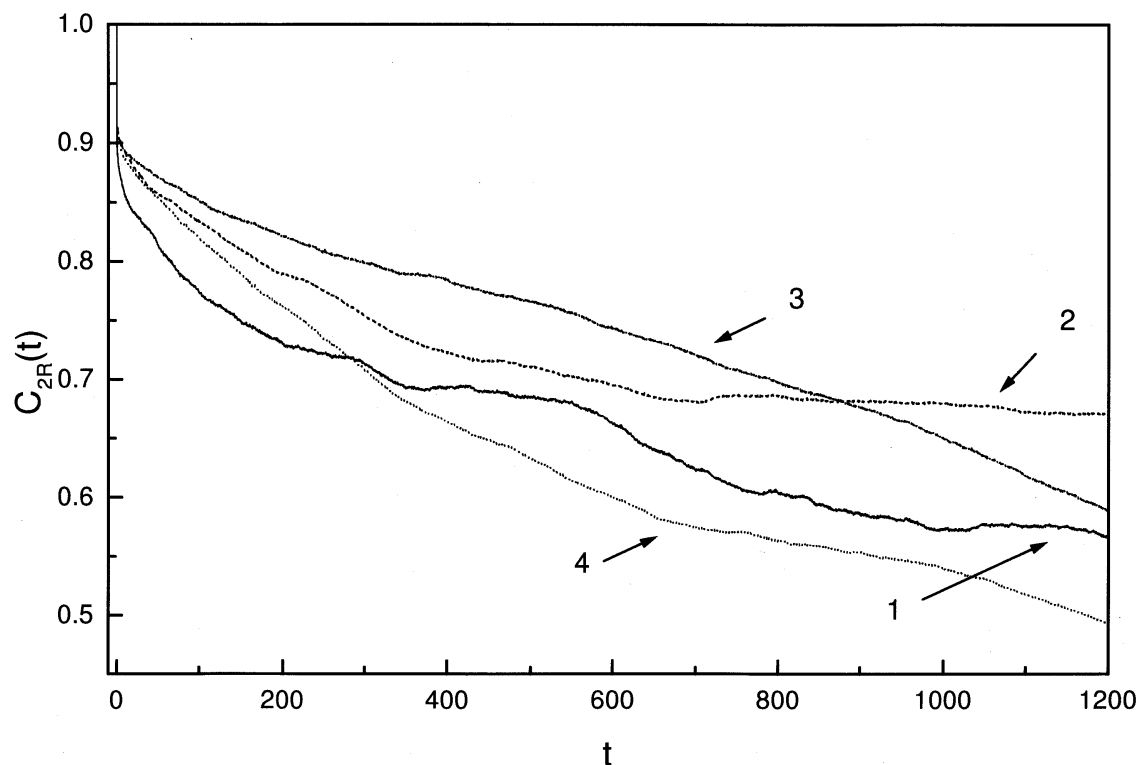


Figure 11. The orientational correlation function $C_{2R}(t)$, is plotted against reduced time, individually, for 4 ellipsoids. The plot shows the presence of heterogeneous dynamics present in the binary mixture, as probed by the orientational dynamics of the ellipsoid. The solid line is for ellipsoid 1, the dashed line is for ellipsoid 2, the dashed-dot line is for ellipsoid 3 and the dotted line is for ellipsoid 4. The study is performed at $T^* = 0.8$ and $P^* = 10.0$.

rotation will be large and thus it will probe a more homogeneous solvent dynamics. To observe the heterogeneity, the time scale of rotational dynamics should be in between the time scale of the dynamics of (A) and (B).

8. Beyond the classical transport laws of electrochemistry

The classical transport laws and theories of electrochemistry have been widely applied to understand the effects of ion concentration on the diffusion of ions, ionic conductivity of electrolytes and the viscosity. The most celebrated among these is the Debye–Huckel–Onsager (DHO) law which predicts a square root concentration dependence of ion conductance⁶⁹. There are two other laws which are often discussed in the literature. These are the Debye–Falkenhagen (DF) theory of the frequency dependence of ionic conductivity. One often refers to Debye–Falkenhagen (DF) effect as the anomalous rise of conductivity with frequency at low frequencies which follows from the Debye–Falkenhagen theory. Another well-known theory is the Falkenhagen–Onsager–Fuoss (FOF) theory of the concentration dependence of the excess viscosity of ionic solutions. This theory correctly explains the rise of viscosity with concentration in the limit of *very low* ion concentration.

The classical derivations of these transport laws were highly non-trivial, often involving astute use of electrohydrodynamics and irreversible thermodynamics – the 1932 article by Onsager and Fuoss is a case in point⁷⁰. Not only have these laws been hailed as the intellectual triumphs of the last century, they have also been tremendously successful in explaining concentration dependence of conductivity at low ion concentration. However, these laws are certainly not perfect. They are valid only at *very low* ion concentration and are applicable for strongly dissociative salt solutions like NaCl and KCl in water. Both the successes and the limitations of these classical theories can be traced back to the basic conceptual framework on which they are based. This conceptual framework has two basic ingredients. First, the solvent is treated as a structure-less continuum with a given static dielectric constant and viscosity. Second, there exists an ion atmosphere of net opposite charge around each ion due to ion attraction. The radius of this ion atmosphere is the Debye length (I_D) which has an inverse square root dependence on the concentration of the ions. The validity of the classical laws is crucially dependent on the value of the Debye length. When the Debye length is much larger than the molecular lengths (such as the radius of ions), then the classical description where the solvent is treated as a *dielectric continuum* is valid. The equilibrium theories based on this assumption are often referred to as ion attraction theory or Debye–Huckel theory.

There have been several attempts to extend the Debye–Huckel–Onsager limiting law of conductance to higher ion concentrations. The most notable among them is the work of Friedman and coworkers⁷¹ and of Bernard, Blum, Turq (BBT) and coworkers⁷². In the former approach, the motion of an ion is described as a Brownian particle in the force-field of other ions of the system. The force-field is described in terms of ion pair correlation functions. A dynamical theory at Smoluchowski level is used to calculate the transport properties. In the approach of Bernard, Blum and Turq, one uses the formal expressions of the transport properties in terms of ionic pair correlation functions derived earlier by Onsager and Fuoss by using the continuity equation approach. BBT provided explicit expressions for the calculation of transport properties as a function of the equilibrium ionic pair correlation functions stemming from modern statistical mechanical theory of liquids such as HNC or MSA. Also, the difference between the self-diffusion and the conductivity was explicitly taken into account in the later work by Turq and coworkers⁷². Expressions derived in both the two latter approaches reduce to the DHO law in the limit of low concentration. Both the approaches do considerably better than the original DHO expression at higher concentrations.

Computer simulation is a complementary method to study transport phenomena in ionic solutions⁷³. Among the simulation techniques, the method of molecular dynamics (MD) allows us to study the structural and dynamical properties of both ions and solvent molecules at Born–Oppenheimer level of description. This technique has been used to study self-diffusion and conductivity of simple model solutions such as ions in Stockmayer liquid and also of more realistic solutions such as NaCl and KCl in water at finite concentrations. However, the implementation of this technique for ionic solutions is computationally very costly because of the multiplicity of components, the long-range nature of the interparticle interactions and the very long run that is required to obtain statistically meaningful averages. This is why a great majority of the simulation studies have used techniques of stochastic simulations which allow a simplification of the mathematical description of the solutions. In these methods, the solution can be treated at the McMillan–Mayer level of description where solvent particles are not considered explicitly, they are represented by a dielectric continuum and the solute particles interact through solvent averaged potentials. Brownian Dynamics (BD) and Langevin Dynamics (LD) are two of these stochastic simulation methods that have been employed to calculate the self-diffusion and conductivity of various aqueous ionic solutions and reasonably good agreement has been found with experimental results. These studies also showed the breakdown of Debye–Huckel and Debye–Huckel–Onsager classical laws at finite concentrations. No

simulation study has yet been carried out to calculate the viscosity of ionic solutions.

There is one valuable lesson to be learned from the above studies which is that the dielectric continuum model itself may be trusted to concentration as high as 1 M solution while the original DHO law breaks down at 0.01 M. However, this relative success may be limited only to the calculation of diffusion and conductivity and might not be extendable to other transport properties, like viscosity. In addition, there are several aspects of the earlier theoretical approaches which require further improvement. First, these theories are not fully microscopic in the sense that they are not based on the time correlation function (tcf) formalism of transport properties. Also, these theories are not fully self-consistent.

Recently, we have been able to derive all the three classical transport laws using the basic concepts of mode coupling theory and the time-dependent density functional theory^{11,74-77}. The resulting expressions for conductivity and viscosity involve the dynamic structure factor and the current-current correlation function. In fact, the ion atmosphere term is shown to correspond to dynamic structure factor corresponding to charge density while electrophoretic term corresponds to tcf of charge density current term. When microscopic expressions are evaluated, agreement at par with earlier theories are found for electrolyte conductance. This approach also provides microscopic expressions for the frequency dependence of conductivity and of the excess viscosity of an electrolyte solution.

9. Conclusion

We have summarized above some of the contributions we have made in several different areas of liquid state dynamics. At present we are pursuing work in the area of supercooled liquid and protein folding. In particular, we found that simple models of binary mixtures can describe many different physical phenomena. Thus, similar kind of models of binary mixture can describe viscosity anomaly, hopping transport in supercooled liquids and collapse of a segment of a protein into a well-defined structure. This diversity of binary mixtures comes from the existence of several energy and length scales which give rise not only to frustration (as in supercooled liquids), but also to structure selection, as in protein folding. We are also attempting to develop a fully molecular theory of electrolyte conductance, by treating a three-component system. The statistical mechanics of such a system is rather complicated, but required to describe the complex dynamics of concentrated electrolyte solutions.

1. Marcus, R. A. and Sutin, N., *Biochim. Biophys. Acta*, 1995, **811**, 275.

2. Zewail, A. H. (ed.), *Femtochemistry: Ultrafast Dynamics of the Chemical Bond*, World Scientific, Singapore, 1994.
3. Fleming, G. R. and Wolynes, P. G., *Phys. Today*, 1990, **43**, 36.
4. Voth, G. A. and Hochstrasser, R. M., *J. Phys. Chem.*, 1996, **100**, 13034.
5. Fleming, G. R., *Chemical Applications of Ultrafast Spectroscopy*, Oxford, New York, 1986, chapter 6.
6. Hynes, J. T., in *The Theory of Chemical Reactions* (ed. Baer, M.), Chemical Rubber Publ. Co., Boca Raton, FL, 1985, vol. 4.
7. Hynes, J. T., *Annu. Rev. Phys. Chem.*, 1985, **36**, 573.
8. Mukamel, S., *Principles of Nonlinear Spectroscopy*, Oxford, New York, 1995.
9. Rossky, P. J. and Simon, J. D., *Nature*, 1994, **370**, 263.
10. Bagchi, B., *Annu. Rev. Phys. Chem.*, 1989, **40**, 115.
11. Bagchi, B. and Chandra, A., *Adv. Chem. Phys.*, 1991, **80**, 1.
12. Bagchi, B. and Biswas, R., *Adv. Chem. Phys.*, 1999, **109**, 207 and references therein.
13. Chandra, A. and Bagchi, B., *J. Phys. Chem.*, 2000, **B104**, 9067.
14. Zwanzig, R., *Nonequilibrium Statistical Mechanics*, Oxford, New York, 2001.
15. Marcus, R. A., *J. Chem. Phys.*, 1956, **24**, 966, 979.
16. Marcus, R. A., *Annu. Rev. Phys. Chem.*, 1964, **15**, 155.
17. Heitele, H., *Angew. Chem. Int. Ed. Engl.*, 1993, **32**, 359.
18. Zusman, L. D., *Chem. Phys.*, 1980, **49**, 295; 1983, **80**, 29.
19. Hynes, J. T., *J. Phys. Chem.*, 1986, **90**, 3701.
20. Efrima, S. and Bixon, M., *J. Chem. Phys.*, 1979, **70**, 3531.
21. Bixon, M. and Jortner, J., *Chem. Phys.*, 1993, **176**, 467.
22. Bixon, M., Jortner, J. and Verhoeven, J. W., *J. Am. Chem. Soc.*, 1994, **116**, 7349.
23. Jortner, J. and Bixon, M., *Ber. Bunsenges Phys. Chem.*, 1995, **99**, 296.
24. Jortner, J. et al., *Chem. Phys. Lett.*, 1995, **205**, 451.
25. Walker, G. C., Akesson, E., Johnson, A. E., Levinger, N. E. and Barbara, P. F., *J. Phys. Chem.*, 1992, **96**, 7859.
26. Akesson, E., Johnson, A. E., Levinger, N. E., Walker, G. C., DuBrail, T. P. and Barbara, P. F., *J. Chem. Phys.*, 1992, **96**, 7859.
27. Bagchi, B. and Gayathri, N., *Adv. Chem. Phys.*, 1991, **107**, 1.
28. Roy, S. and Bagchi, B., *J. Phys. Chem.*, 1994, **98**, 9207.
29. Roy, S. and Bagchi, B., *J. Chem. Phys.*, 1995, **102**, 7937.
30. Aldrin Denny, R., Bagchi, B. and Barbara, P. F., *J. Chem. Phys.*, **115** (in press).
31. Barbara, P. F., Walker, G. C. and Smith, T. R., *Science*, 1992, **256**, 975.
32. Oxtoby, D. W., *Adv. Chem. Phys.*, 1981, **47**, 487.
33. Oxtoby, D. W., *Annu. Rev. Phys. Chem.*, 1981, **32**, 77.
34. Tominaga, K. and Yoshihara, K., *Phys. Rev. Lett.*, 1995, **74**, 3061.
35. Gayathri, N. and Bagchi, B., *J. Phys. Chem.*, 1999, **A103**, 9579.
36. Gayathri, N. and Bagchi, B., *Phys. Rev. Lett.*, 1999, **82**, 4851.
37. Herzfeld, K. F. and Litovitz, T. A., *Absorption and Dispersion of Ultrasonic Waves*, Academic, New York, 1959.
38. Skinner, J. L., Egorov, S. A. and Everitt, K. F., in *Ultrafast Infrared and Raman Spectroscopy* (ed. Fayer, M.), Marcel Dekker, New York, 2000.
39. Berne, B. J., Tuckerman, M. E., Straub, J. E. and Bug, A. L. R., *J. Chem. Phys.*, 1990, **93**, 5084.
40. Goodyear, G., Larsen, R. E. and Stratt, R. M., *Phys. Rev. Lett.*, 1996, **76**, 243.
41. Biswas, R., Bhattacharyya, S. and Bagchi, B., *J. Chem. Phys.*, 1998, **108**, 4963.
42. Miyazaki, K., Srinivas, G. and Bagchi, B., *J. Chem. Phys.*, 2001, **114**, 6276.
43. Bagchi, B., Srinivas, G. and Miyazaki, K., *J. Chem. Phys.*, 2001, **115**.
44. Kirkwood, J. C. and Buff, F. P., *J. Chem. Phys.*, 1951, **19**, 774.
45. Qunfang, L. and Yu-Chun, H., *Fluid Phase Equilibria*, 1999, **154**, 153 (and references therein).

46. Pal, A. and Daas, G., *J. Mol. Liq.*, 2000, **84**, 327.
47. Beddard, G. S., Doust, T. and Hudales, J., *Nature*, 1981, **294**, 145.
48. Chandra, A. and Bagchi, B., *J. Chem. Phys.*, 1991, **94**, 8367.
49. Bagchi, B. and Chandra, A., *J. Chem. Phys.*, 1992, **97**, 5126.
50. Kob, W. and Andersen, H. C., *Phys. Rev. E*, 1995, **51**, 4626.
51. Kob, W. and Andersen, H. C., *Phys. Rev. Lett.*, 1994, **73**, 1376.
52. Sastry, S., Debenedetti, P. G. and Stillinger, F. H., *Nature*, 1998, **393**, 554; Sastry, S., *Phys. Rev. Lett.*, 2000, **85**, 590.
53. Sastry, S., *Nature*, 2001, **409**, 164.
54. Srinivas, G., Mukherjee, A. and Bagchi, B., *J. Chem. Phys.*, 2001, **114**, 6220.
55. Mukherjee, A., Srinivas, G. and Bagchi, B., *Phys. Rev. Lett.*, 2001, **86**, 5926.
56. Mukherjee, A. and Bagchi, B., *J. Phys. Chem.*, 2001, **B105**, 9581.
57. Bhattacharyya, S. and Bagchi, B., *J. Chem. Phys.*, in press.
58. Bhattacharyya, S., Mukherjee, A. and Bagchi, B., *Phys. Rev. Lett.*, submitted.
59. Bagchi, B. and Bhattacharyya, S., *Adv. Chem. Phys.*, 2001, **116**, 67.
60. Srinivas, G., Bhattacharyya, S. and Bagchi, B., *J. Chem. Phys.*, 1999, **110**, 4477.
61. Biswas, R., Bhattacharyya, S. and Bagchi, B., *J. Phys. Chem.*, 1998, **B102**, 3552.
62. Ravichandran, S. and Bagchi, B., *J. Chem. Phys.*, 1999, **111**, 7505.
63. The potential has been developed and tested in collaboration with Dr A. Perera of LPTL, Univ. P. et M. Curie, Jussieu, Paris 75252 (private communication). This potential was used in ref. 62 and shown to give consistent results.
64. Ediger, M. D., Angell, C. A. and Nagel, S. R., *J. Phys. Chem.*, **100**; Cicerone, M. T. and Ediger, M. D., *J. Chem. Phys.*, 1996, **104**, 7210; Cicerone, M. T. and Ediger, M. D., *J. Chem. Phys.*, 1996, **103**, 5684; Cicerone, M. T., Blachburn, F. R. and Ediger, M. D., *J. Chem. Phys.*, 1995, **102**, 471; Cicerone, M. T., Blachburn, F. R. and Ediger, M. D., *Macromolecules*, 1995, **28**, 8224; Heuberger, G. and Sillescu, H., *J. Chem. Phys.*, 1996, **100**, 15255.
65. Wolynes, P. G., *Proc. Natl. Acad. Sci. USA*, 1997, **94**, 11037; Brooks III, C. L., Gruebele, M., Onuchic, J. N. and Wolynes, P. G., *Proc. Natl. Acad. Sci. USA*, 1998, **95**, 11037.
66. Kirkpatrick, T. R., Thirumalai, D. and Wolynes, P. G., *Phys. Rev.*, 1989, **A40**, 1045.
67. Murarka, R. and Bagchi, B., *J. Chem. Phys.* (in press).
68. Bosse, J. and Kaneko, Y., *Phys. Rev. Lett.*, 1995, **74**, 4023.
69. Glasstone, S., *An Introduction to Electrochemistry*, LEP, New York, 1942, Ch. III.
70. Onsager, L. and Fuoss, R. M., *J. Phys. Chem.*, 1932, **36**, 2689.
71. Altenberger, A. R. and Friedman, H. L., *J. Chem. Phys.*, 1983, **78**, 4162; Zhong, E. C. and Friedman, H. L., *J. Phys. Chem.*, 1988, **92**, 1685.
72. Bernard, O., Kunz, W., Turq, P. and Blum, L., *J. Phys. Chem.*, 1992, **96**, 398; *ibid* 1992, **96**, 3833; Turq, P., Blum, L., Bernard, O. and Kunz, W., *J. Phys. Chem.*, 1995, **99**, 822.
73. Bagchi, B. and Biswas, R., *Acc. Chem. Res.*, 1998, **31**, 181.
74. Chandra, A., Biswas, R. and Bagchi, B., *J. Am. Chem. Soc.*, 1999, **121**, 4082.
75. Chandra, A. and Bagchi, B., *J. Chem. Phys.*, 1999, **110**, 10024.
76. Chandra, A. and Bagchi, B., *J. Chem. Phys.*, 2000, **112**, 1876.
77. Chandra, A. and Bagchi, B., *J. Chem. Phys.*, 2000, **113**, 3226.

ACKNOWLEDGEMENTS. The work reported here was carried out in collaboration with Dr R. Aldrin Denny, Dr Sarika Bhattacharyya, Dr Ranjit Biswas, Prof. A Chandra, Dr N. Gayathri, Mr Arnab Mukherjee, Mr Rajesh Murarka, Prof. Srabani Roy, Mr G. Srinivas and Ms R. Vasanthi. It is pleasure to thank Prof. Graham Fleming, Prof. Casey Hynes, Prof. Kankan Bhattacharyya, Prof. Paul Barbara, Dr Kunimasa Miyazaki, Prof. Iwao Ohmine, Prof. Peter Rossky for discussions and correspondence. It is a pleasure to thank Dr Srikanth Sastry for many useful discussions both about (NPT) simulations and binary mixtures. This work was supported in parts by grants from the Department of Science and Technology (DST), and the Council of Scientific and Industrial Research (CSIR), India.